Validation of Anode Current Distribution Measured by a Smart Individual Anode Monitoring System

Jing Shi[1], Choon-Jie Wong[2], Maitha Faraj[3], Nadia Ahli[4], Jie Bao[5], Barry Welch[6], Hassan Alhayas[7] and Mohamed Mahmoud[8]

1. Lead Engineer
3, 8. Manager
4. Senior Manager
7. Senior Engineer
Emirates Global Aluminium, Dubai, U.A.E.
2. Postdoctoral Fellow
5. Professor
6. Emeritus Professor
University of New South Wales, Sydney, Australia
Corresponding author: mfaraj@ega.ae
https://doi.org/10.71659/icsoba2024-al045

Abstract

Nowadays, larger aluminium reduction cells are constructed with reduced bath-to-anode volume ratios to operate at higher currents and lower anode cathode distance. With aims of increasing production efficiency while lowering energy consumption, the significance of spatial variability in process variables within the cell has intensified. While conventional measurements such as cell voltage and line current fail to depict localised cell conditions, real-time individual anode distribution measurements offer insights into monitoring the spatial dynamics of process variables within the cell. This paper introduces the continuous measurement of anode current distribution through a smart Individual Anode Monitoring (IAM) system. To validate the IAM signals, a comprehensive campaign was conducted involving direct measurements of voltage drop from individual anode rods utilising C-clamps at a designated aluminium smelting cell. This validation process spans one complete anode change cycle, enabling the comparison of anode currents across various operational conditions, including idle shifts, routine manual practices, and other non-routine operations.

Keywords: Anode monitoring, Anode current distribution, Signal calibration and validation, Operational efficiency.

1. Introduction

Monitoring individual anode current signals in the Hall-Héroult cells represents a significant advancement over conventional techniques, greatly enhancing the understanding of localised variations within the electrolysis cell. Traditionally, monitoring frameworks have focused on measuring overall line current and cell voltage [1, 2], providing a snapshot of general cell conditions, such as average alumina concentration. However, these metrics are insufficient for detecting specific localised disparities or operational faults, particularly as the industry shifts towards higher electrical loads.

Technological developments have led to larger anode sizes without a corresponding increase in the volume of molten bath, making the assumption of uniform conditions across the cell increasingly untenable [3]. This mismatch introduces complexities in maintaining consistent cell performance. Additionally, modern practices aimed at reducing energy consumption often involve decreasing the anode-cathode distance in high-current cells. This reduction restricts bath mixture flow, leading to inadequate mixing and uneven property distribution within the cell.

These factors make detailed monitoring of individual anode currents essential for optimal Hall-Héroult cell operation [4-7].

The interaction between anode currents and their specific local environments within a Hall-Héroult cell is both critical and intricate. Each anode-cathode pathway is characterised by distinct bath compositions and temperatures, significantly influencing the distribution of regulated line current among the pathways. This distribution is affected by several key electrical parameters, including local reversible potential, cell overpotentials, and the ohmic potential drop along each path. These factors highlight the complexity of achieving balance and uniformity in cell operation. [8-10] Anode currents not only influence current distribution but also facilitate localised electrolytic reactions and generate ohmic heating within their respective pathways. This activity is crucial for the cell's chemistry and thermal dynamics, impacting overall efficiency and productivity. Measuring these individual currents provides a detailed visualisation of spatial variations within the cell [11-13], allowing operators to predict and adapt to potential dynamic changes, thereby enhancing the cell's operational stability and performance over time [14-17].

This paper summarises the validation results of a novel approach for measuring individual anode currents in real-time monitoring and control of the Hall-Héroult process. Unlike traditional methods that measure currents directly from the anode rod, this method captures readings from the anode beam, enhancing sensor longevity during various operational stages, including anode replacement.

2. Instrumentation and Installation

2.1 Sensor Architecture and Design

We have designed and manufactured an IAM system in-house, some of the details of which were published elsewhere [6]. The system accurately determines the current I flowing along a conductor by measuring the voltage drop V across a known distance L on the conductor with cross-sectional area A. The system also measures the conductor temperature T to compensate for small changes in resistance due to temperature variations. For a conductor with resistivity linear to temperature, its current is calculated with

$$I = \frac{A}{(\rho_1 T + \rho_2)L} V, \tag{1}$$

where ρ_1 and ρ_2 are the resistivity coefficients. Compared to other non-intrusive measurement systems, this method offers a direct and low-cost measurement solution using Ohm's Law.

Based on years of experience developing previous iterations of IAM system, our latest design focuses on superior signal quality and system robustness for scalable commercial deployments. The IAM system measures current from the anode beam instead of the anode rod, allowing uninterrupted measurements through operations such as anode change and beam raising. A dedicated digital sensor measures and processes voltage and temperature data at each beam location at over 100 Hz, enabling distributed processing. As each sensor has its own microprocessor and can function autonomously, they can independently adjust their signal amplifier gain, achieving a high signal-to-noise ratio even for beam locations with naturally small signal magnitude. The sensors, orchestrated by a communication unit, communicate digitally through robust industry-standard Controller Area Network (CAN) protocol to minimise signal degradation and interference associated with analogue transmission used by simpler IAM systems.

Figure 1 shows the installation layout of the IAM system, featuring smart sensors in a daisy-chain configuration along a unified communication line. The sensors are bolted on the top of the anode beam and covered in a channel for protection, as shown in Figure 2. Its versatile design ensures compatibility with various cell technologies, making it robust for different operational environments.

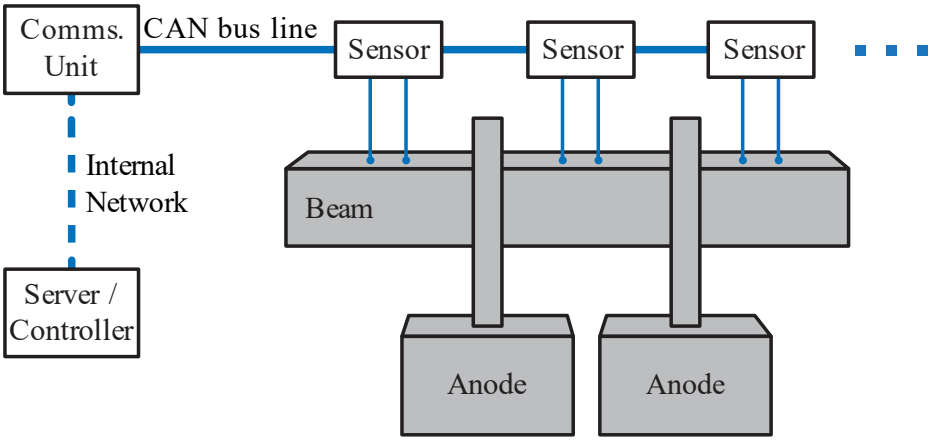

Figure 1. Schematic of the IAM system.

Figure 2. Sensors on the anode beam are enclosed in a channel for additional protection against dust particulates and moisture.

The measured IAM signals are processed and stored locally on EGA servers and datastores, eliminating cloud computing costs and data exposure risks associated with other IAM systems. Figure 3 shows a custom interface software developed by EGA to display raw measurements from the IAM system. Some readings are negative due to the direction of current flow in the anode beam. Beam currents are calculated from the raw data with Eq. 1, from which anode currents are obtained and plotted on a separate interface. These interfaces can be accessed anywhere on desktop computers and tablet devices within EGA, as well as from company laptops via enterprise VPN when teleworking. By monitoring anode current distribution, the system improves operational management and promptly detects anomalies such as local low concentration of alumina, said to be the cause of perfluorocarbon co-evolution, and feeder blockages. It thus helps to optimise cell performance.

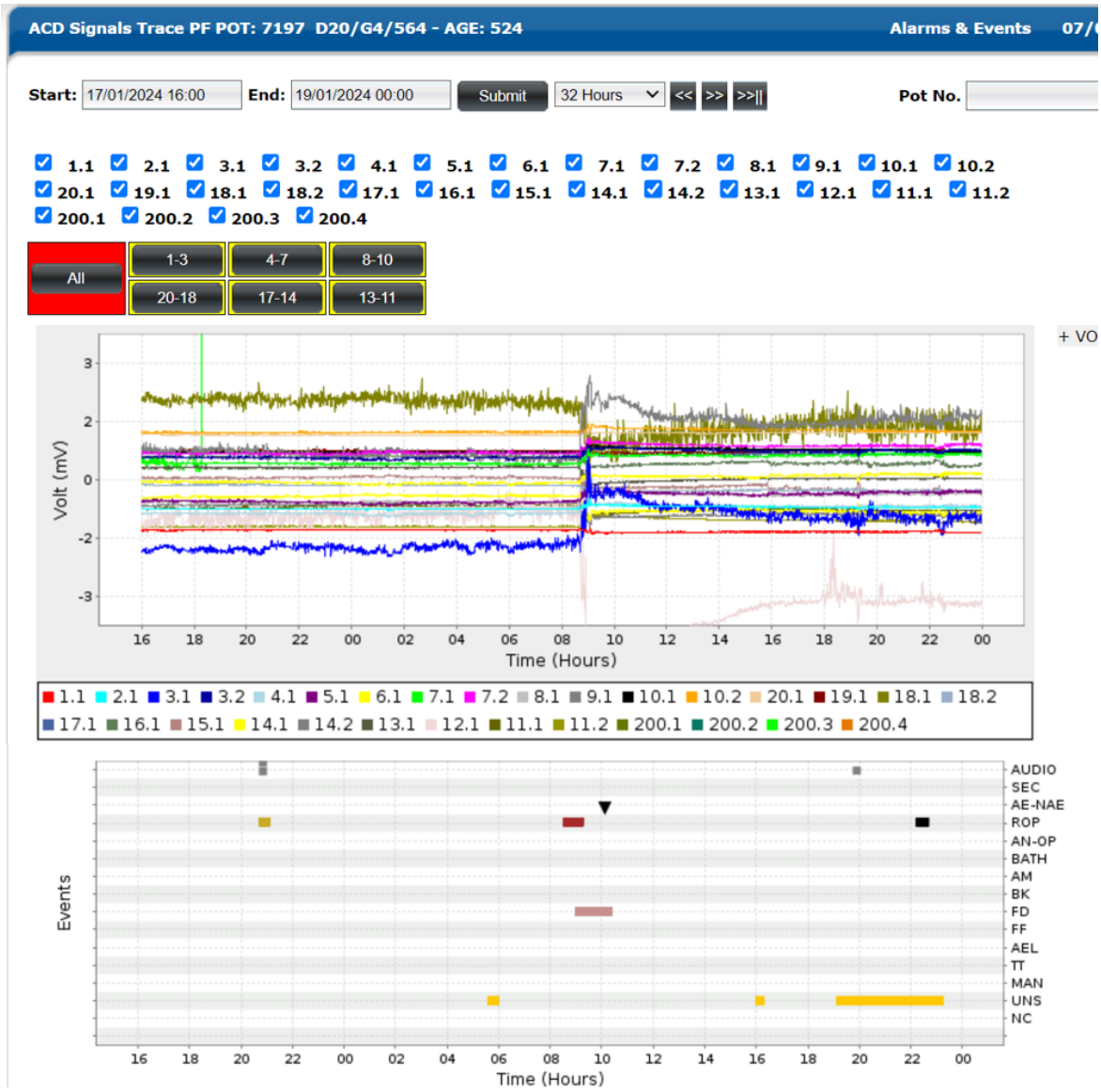

Figure 3. EGA pot monitoring interface showing raw measurements from IAM system, aligned with pot activities and operations. An anode change occurred at 9AM.

2.2 Validation Instrumentation

The measurement technique is based on a tried and tested principle with successful outcomes published in the literature [6]. Previous iterations of our IAM systems have also been deployed successfully across a full potline section in EGA. While our current IAM system iteration has been validated on EGA DX cell technology, this paper describes the positive outcomes on EGA D20 cell technologies, showing the versatility of the system on various cell technologies.

The data collected from two commercial D20 aluminium reduction cells were used in this validation study. For validation purposes, the distribution of anode currents was continuously monitored with C-clamps on each anode rod to verify IAM signal accuracy (Figures 4-5). Data from an entire anode change cycle were continuously recorded, enabling detailed analysis of each anode behaviour, especially during anode setting operations. This comprehensive data collection is crucial for evaluating the IAM system precision and reliability under actual operational conditions.

The vertical placement of the C-clamp on the anode rod is important for accuracy of rod current readings. If the C-clamps were positioned too high on the anode rod, the anode current may not be flowing vertically down. However, C-clamps that are positioned too low will be subject to damages as beam raising activities are performed, leading to signal losses. After the C-clamps were installed, their readings were quickly validated against a handheld probe tool that outputs instantaneous rod current measurements.

Figure 4. C-clamp installed on an anode rod.

Figure 5. C-clamps installed on the anode rods of cell upstream side.

3. Comparisons of Anode Current Measurements

To conduct a comprehensive analysis, data from an entire anode change cycle were examined, comparing IAM signals with those from C-clamps under various conditions. Understanding fluctuations in anode current distribution is crucial for tasks like anode setting, beam raising, and metal tapping. This analysis identifies deviations that might affect system performance. Initially, data are presented over the full cycle duration to provide a clear view of the IAM system's performance, highlighting any trends or anomalies. This thorough examination assesses the IAM system's robustness and reliability in different operational scenarios.

3.1 Overall Comparison – One Complete Anode Change Cycle

3.1.1 Experimental Trial at the 1st Cell

The current flowing through all anodes were measured. Individually, the magnitude of anode current represents the rate of local material generation and consumption, and local heat generation. When compared as a whole, the distribution among the anodes informs of the local path impedances arising from local cell conditions. However, for clarity in our illustrations of the validated results, we plot and discuss in this paper only the signals from a few selected anodes as an example (Figure 6). In all figures, the raw IAM signal is plotted as blue lines, while after calibration, the signals are plotted as black dashed lines. The calibration corrects for variances in pickup pin distances, beam cross-sectional area, uniformity in current density, among other uncertainties introduced during the installation process. The calibration can be conducted with a system of simultaneous equations for which the calibration factors, α and β, are solved simultaneously. For example,

- Equations 2 and 3 are the calibrated version of Equation 1.
- Equations 4 and 5 are the anode currents, showing that one beam current is used for the calculation of two anode currents, thereby necessitating a simultaneous solution.
- Equation 6 denotes the requirement that anode currents must sum up to the line current.

$$I_1 = \alpha_1 \frac{A}{(\rho_1 T_1 + \rho_2)L} V_1 + \beta_1, \quad (2)$$

$$I_2 = \alpha_2 \frac{A}{(\rho_1 T_1 + \rho_2)L} V_2 + \beta_2, \quad (3)$$

$$\vdots$$

$$I_{\text{an1}} = I_1 - I_2, \quad (4)$$

$$I_{\text{an2}} = I_2 - I_3, \quad (5)$$

$$\vdots$$

$$I_{\text{line}} = I_{\text{an1}} + I_{\text{an2}} + \cdots. \quad (6)$$

Finally, the C-clamp signals are plotted as orange lines, for validation purposes. It is noted that the rod temperature used to calculate C-clamp currents are measured only once a day. While this introduces some error particularly after anode change operations where the temperature varies over time, the comparison is still useful to cross-check IAM signals.

For the D20 cells with a line current of 270 kA, the average anode current is 13.5 kA. Due to frequent anode changes, the anode current fluctuates around this value. Previous studies [8] show that anode current changes the most when neighbouring anodes are changed, showing that the distribution of current is not even. This is also seen as fluctuations in the anode currents in Figure 6 with period of 1–2 days.

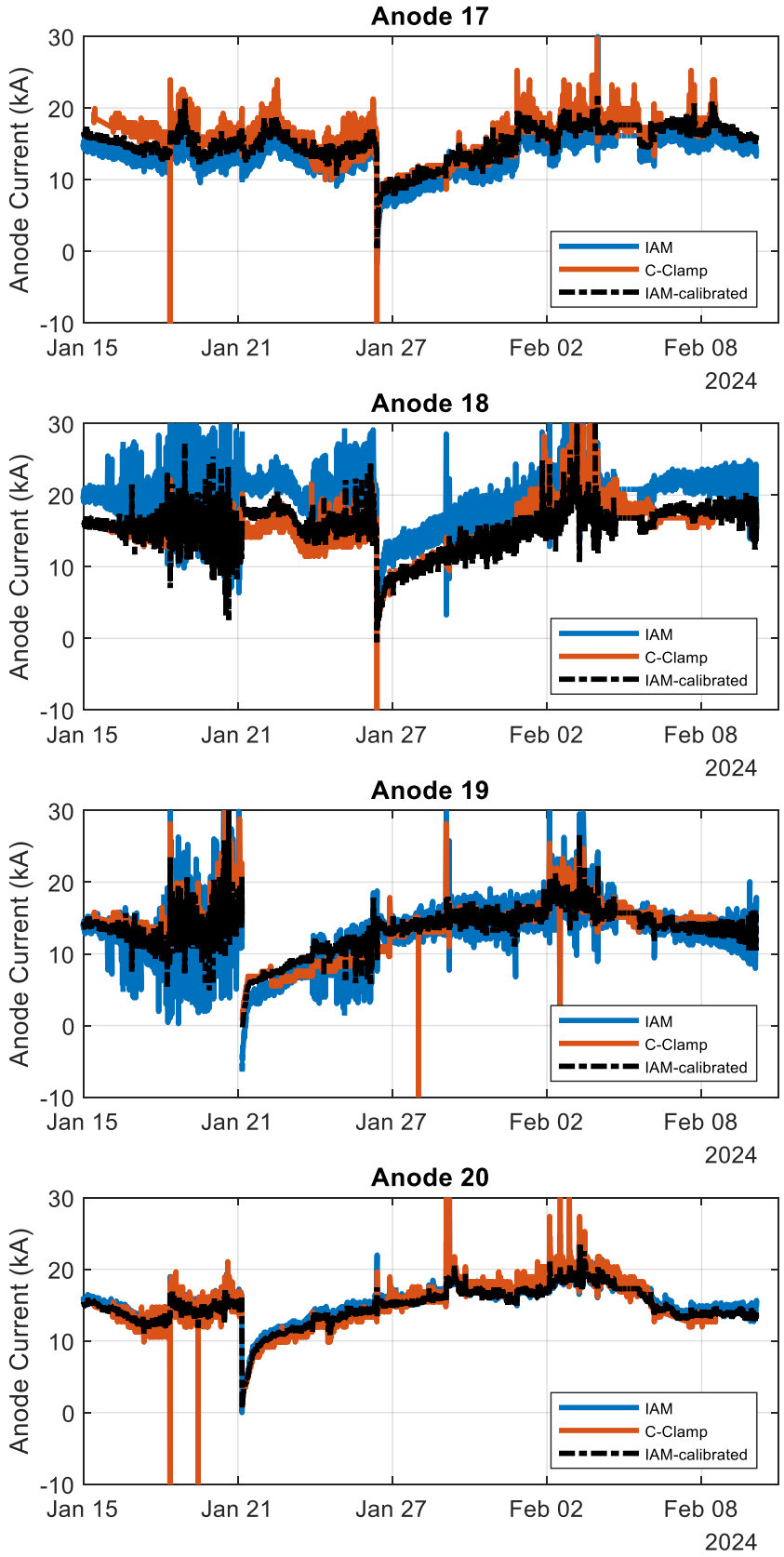

Figure 6. Comparison of C-clamp signal and IAM signal from anode 17 to anode 20 of the first cell.

3.1.2 Experimental Trial at the 2nd Cell

Similarly, the IAM signal from the second cell showed excellent alignment with the C-clamp signal after calibration (Figure 7). However, a notable discrepancy in signals from specific anodes was observed, primarily due to a failure at the pickup point. This issue, identified during the validation campaign, stemmed from a mechanical problem. It was promptly addressed and rectified shortly after detection during the trial phase. The swift resolution of this fault underscores the robustness of the monitoring system's maintenance protocols and its ability to ensure continuous accuracy and reliability in signal measurement under varying operational conditions.

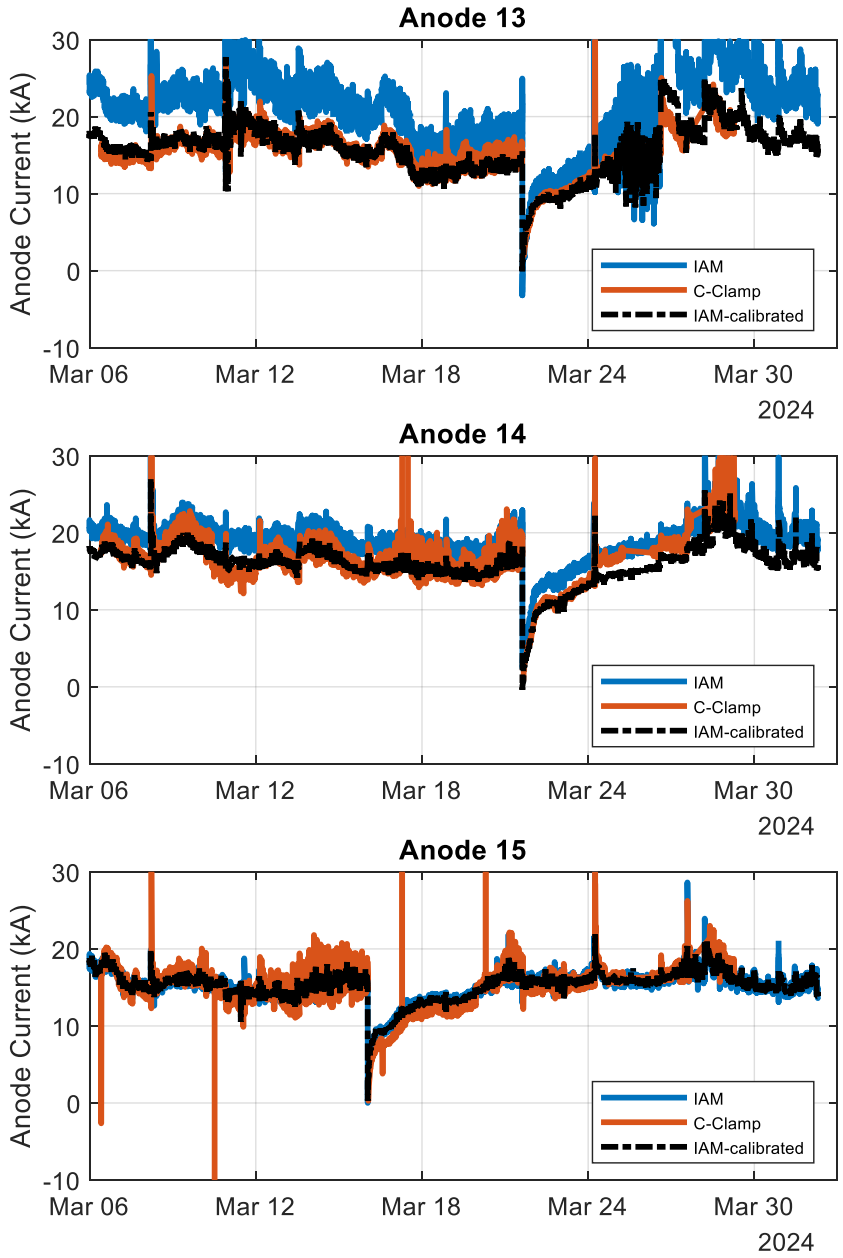

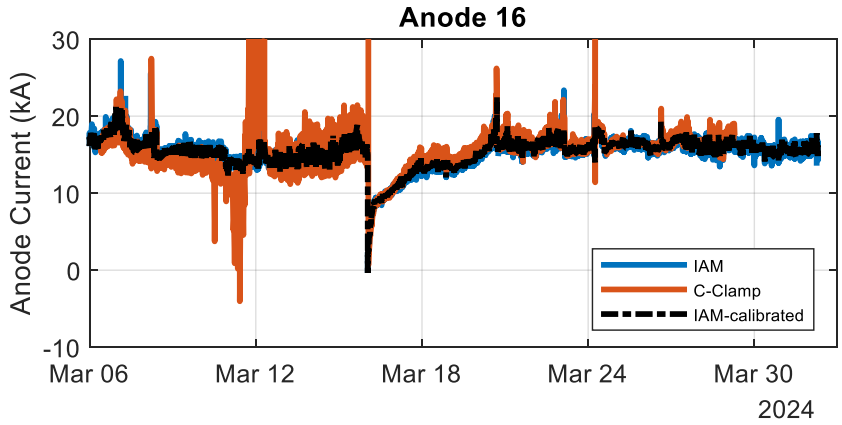

Figure 7. Comparison of C-clamp signal and IAM signal from anode 13 to anode 16 of the second cell.

3.2 Routine Operation – Anode Setting

3.2.1 Experimental Trial at the 1st Cell

To examine the accuracy of the IAM signal during anode setting, the time scale was magnified. This detailed view in Figure 8 shows that the calibrated IAM signal closely aligns with the C-clamp signal, confirming effective calibration. Anodes 15 and 16 were selected to demonstrate the alignment between the IAM signal and the C-clamp signal. Notably, there was significant noise in the anode current around 18:00 h on January 31st, a common issue with older anodes, which are prone to higher noise levels.

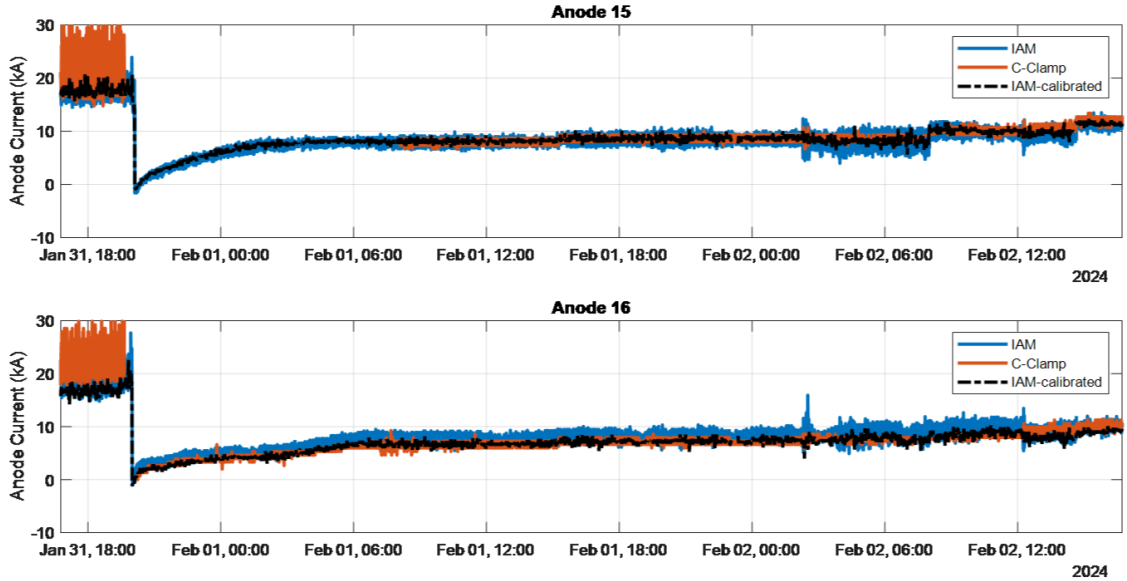

Figure 8. Comparison of C-clamp signal and IAM signal for anodes 15 and 16 during anode setting of the first cell.

3.2.2 Experimental Trial at the 2nd Cell

Similarly, during the anode setting phase, the comparison reveals excellent alignment between the calibrated IAM signal and the C-clamp signal, highlighting the IAM system's effectiveness in capturing precise data (Figure 9). Specifically, at the second cell, the IAM system demonstrates notable improvements in accuracy, attributed to refined pickup point designs and meticulous

sensor installation. These targeted enhancements have not only improved the system's reliability but also its ability to consistently deliver precise readings, reinforcing the operational excellence of the monitoring setup.

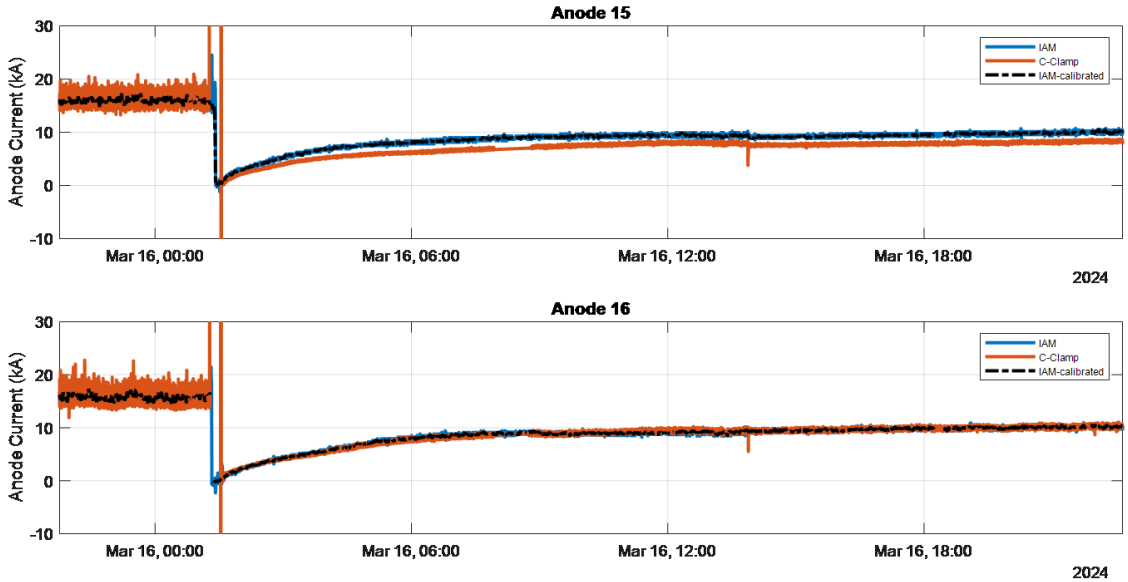

Figure 9. Comparison of C-clamp signal and IAM signal for anodes 15&16 during anode setting of the second cell.

3.3 Routine Operation – Beam Raising

Unlike C-clamps, which must be removed, the IAM system captures data continuously, avoiding interruptions. This advantage streamlines monitoring, minimises disruptions, and reduces manual workload. Continuous data capture enhances operational efficiency and reduces errors during critical maintenance, highlighting the IAM system's pivotal role in improving electrolysis process monitoring.

The data and Figure 10 show how IAM signals behave during the beam raising operation, a critical phase prone to data loss due to anode disengagement. This operation disrupts normal electrical pathways, potentially causing gaps in data continuity. Following beam raising, there is a noticeable increase in anode current distribution variability, effectively captured by the IAM system. This sensitivity reflects the system's responsiveness to operational changes. Enhanced variation in current distribution may result from transient adjustments as the cell returns to normal operation. Monitoring these fluctuations is crucial for understanding cell dynamics and implementing timely corrective actions, underscoring the importance of advanced monitoring systems in maintaining efficient and reliable cell operations.

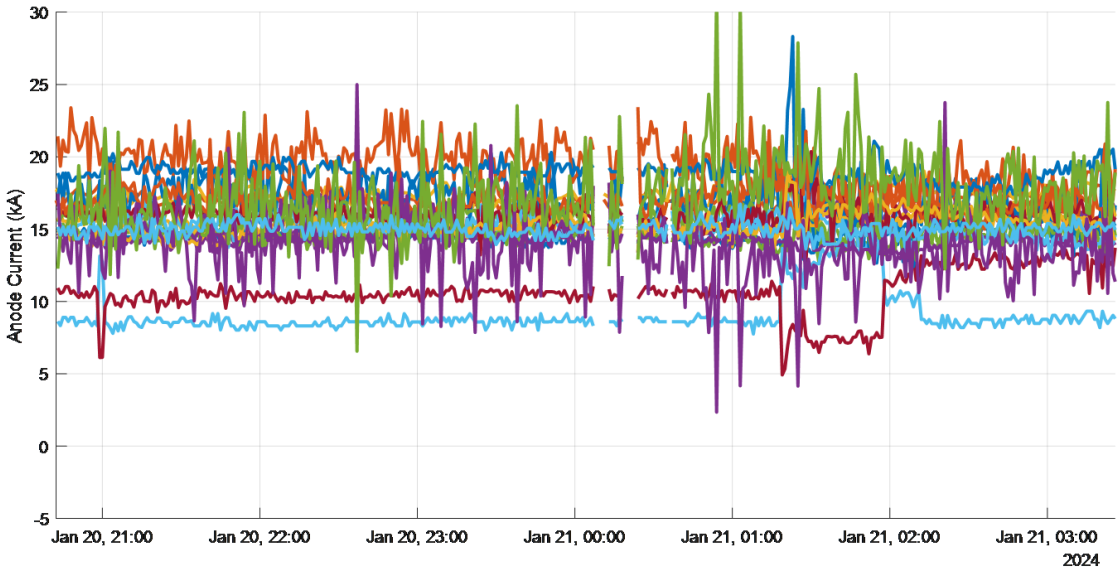

Figure 10. Anode current distribution during beam raising of the first cell.

3.4 Some Specific Event Examples

Figure 11 provides a comprehensive analysis of IAM signal variations during key operational phases: anode change, beam raising, and metal tapping. This visualisation offers valuable insights into system performance across multiple phases.

The data shows robust IAM system performance for two newly installed anodes, with significantly reduced signal noise following anode change. This improvement is crucial as older anodes nearing the end of their service life tend to have increased noise levels due to structural degradation and altered electrical properties. Replacing nearly consumed anodes with new ones typically results in cleaner, more stable signal output.

The clearer, less noisy signals post-anode change confirm the IAM system's reliability in capturing precise variations and its ability to adapt to changing anode conditions. By monitoring these transitions effectively, the IAM system ensures optimal operational control and maintains high process efficiency standards in smelting operations.

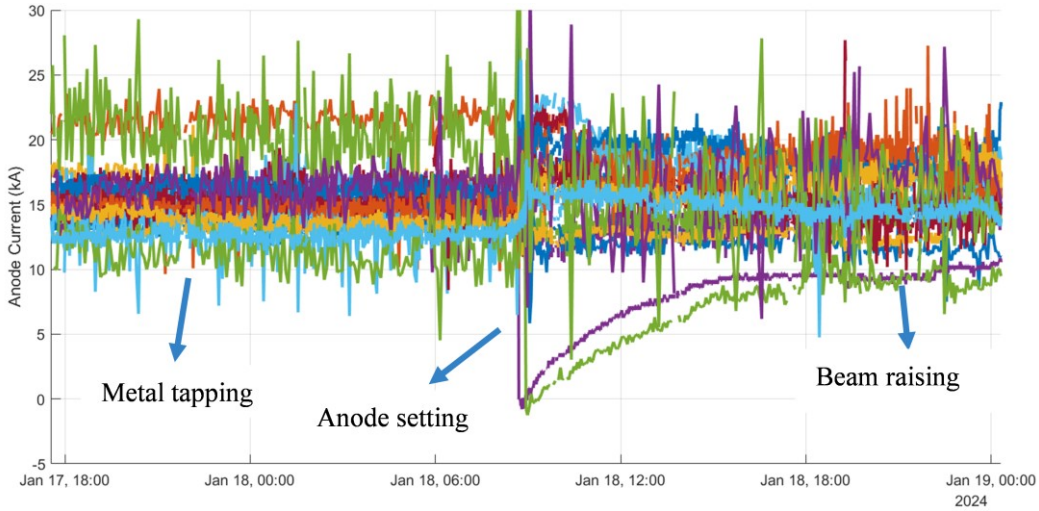

Figure 11. Anode current distribution during multiple events of the first cell.

4. Discussions

This study reaffirms the versatility of the in-house IAM system on various cell technologies. At EGA, the system has been tested on cells ranging from conventional D20 technology to modern high line amperage DX and DX+ Ultra technologies. The IAM system can be retrofitted on existing operating cells without any production downtime, although EGA has now shifted its installation strategy to only target cut-out cells in the interest of workplace safety.

Anode current readings obtained using C-clamps offer the simplest and most direct measurement technique, as signals are obtained directly from anode rods. However, experience from an earlier iteration of our in-house IAM system that measures anode rod signals revealed a lot of challenges. Due to cell operations including anode set, anode check, and beam raising, the signal pickup probes on the anode rods must be removed or repositioned, thus increasing labour costs as well as damages to the probes and anode rods due to increased handling. In the latest iteration of IAM system, the signals are obtained from the beam, allowing uninterrupted signal measurements through all cell operational conditions. The potential drawback is a larger signal reading uncertainty, as an anode current signal is derived from two beam signal readings, each with its own uncertainty. This paper shows that post-calibration, the IAM system offers accurate measurements. The anode current signals are also aligned with operations, for optimising operational efficiency and enhancing decision-making in aluminium smelting operations.

However, we note that our detailed comparison and analysis show that the calibrated IAM signal does not perfectly align with the C-clamp readings. This is attributed to the low frequency reading of anode rod temperature (once a day), which could lead to discrepancies in estimated and actual resistances of the anode rod especially after operations such as anode change. C-clamp readings are also less robust as it is not possible to cross-check individual readings using a set of simultaneous equations — the only test available being that whether all measured anode currents sum up to the line current. Analysis shows that C-clamp measurements can at times deviate up to 10 % from IAM signals, which is consistent with uncertainties in resistivity due to temperature differences. This highlights the importance of temperature measurements, which is built into the IAM system.

5. Conclusions

The validation campaign for the IAM signal was successfully executed with collaborative support from various departments, demonstrating the system's robust functionality across different operational contexts. Throughout this campaign, a complete cycle of anode current distribution data from two pots was meticulously recorded. The results affirm the high accuracy of the IAM signal, which aligns exceptionally well with the C-clamp measurements. This precise correlation underscores the IAM system's reliability in capturing and replicating existing measurement standards. Although the C-clamp measurements at times deviate up to 10%, this is attributed to the low frequency in anode rod temperature measurement, as compared to the continuous beam temperature measurement employed by the IAM system.

Further analysis of the anode current distribution signals during routine operations revealed distinct advantages of the IAM system over traditional C-clamp setups. Notably, the IAM system provides superior data continuity, eliminating gaps typically occurring during manual adjustments with C-clamps. Additionally, the IAM system significantly reduces the time required to gather and process data, enhancing operational efficiency. These improvements are crucial for optimising workflow and increasing productivity by minimising downtime and streamlining monitoring processes. By facilitating more continuous and time-efficient monitoring, the IAM system enhances data accuracy and creates a more streamlined, less labour-intensive operational

environment. These benefits highlight the transformative impact of IAM technology in industrial settings, paving the way for advanced, reliable, and efficient monitoring practices.

6. References

1. Pierre Homsi, Jean-Michel Peyneau, and Michel Reverdy, Overview of Process Control in Reduction Cells and Potlines, *Light Metals* 2000, 739-746.
2. Ya Shuang Gao, Mark P. Taylor, John JJ Chen, and Michael J. Hautus, Operational and control decision making in aluminium smelters. *Advanced Materials Research*, 2011, 201—203, 1632-1641.
3. Marc Dupuis, and Barry Welch, Designing cells for the future–wider and/or even higher amperage?, *ALUMINIUM*, vol. 93, 2017, 45–49.
4. Jeffrey Keniry, and Eugene Shaidulin, Anode signal analysis -- the next generation in reduction cell control*, Light Metals* 2008, 287-292.
5. Ketil A. Rye, Margit Konigsson, and Ingar Solberg, Current Redistribution Among Individual Anode Carbons in A Hall-Heroult Prebake Cell at Low Alumina Concentrations, *Light Metals* 1998, 242-246.
6. Choon-Jie Wong, Jing Shi, Jie Bao, Barry J. Welch, Maria Skyllas-Kazacos, Ali Jassim, Mohamed Mahmoud, and Konstantin Nikandrov, A smart individual anode current measurement system and its applications, *Light Metals* 2023, 43-51.
7. Vinko Potocnik, and Michel Reverdy, History of Computer Control of Aluminium Reduction Cells*, Light Metals* 2021, 591-599.
8. Cheuk Yi Cheung. Anode Current Signals Analysis, Characterization and Modelling of Aluminium Reduction Cells, *Ph.D. thesis*, 2013, School of Chemical Engineering, Faculty of Engineering, the University of New South Wales, Australia.
9. Choon-Jie Wong, Yuchen Yao, Jie Bao, Maria Skyllas-Kazacos, Barry J. Welch, Ali Jassim, Mohamed Mahmoud, and Alexander Arkhipov, Modelling of Coupled Mass and Thermal Balances in Hall-Heroult Cells During Anode Change, *Journal of the Electrochemical Society*, 2021, 168(21):123506.
10. Choon-Jie Wong. Dynamic mass and heat balance model of Hall-Héroult cells: a discretised approach, *Ph.D. thesis*, 2022, School of Chemical Engineering, Faculty of Engineering, the University of New South Wales, Australia.
11. Yuchen Yao, Cheuk-Yi Cheung, Jie Bao, and Maria Skyllas-Kazacos. Monitoring local alumina dissolution in aluminum reduction cells using state estimation, *Light Metals* 2015, 577-581.
12. Yuchen Yao, Cheuk-Yi Cheung, Jie Bao, and Maria Skyllas-Kazacos, Akhmetov Sergey, Jassim Ali, Method for estimating dynamic state variables in an electrolytic cell suitable for the Hall-Heroult electrolysis process, 2017, Patent number WO 2017/141134 A1.
13. Yuchen Yao, and Jie Bao, State and parameter estimation in Hall-Heroult cells using iterated extended Kalman filter, *IFAC-PapersOnLine*, 2018, 51(21):36-41.
14. Choon-Jie Wong, Yuchen Yao, Jie Bao, Maria Skyllas-Kazacos, Barry J. Welch, Ali Jassim, and Mohamed Mahmoud, Discretized Thermal Model of Hall-Heroult Cells for Monitoring and Control, *IFAC-PapersOnLine*, 2021, 54(11):67-72.
15. Jing Shi, Yuchen Yao, Jie Bao, Maria Skyllas-Kazacos, and Barry J. Welch, Multivariable Feeding Control of Aluminum Reduction Process Using Individual Anode Current Measurement, *IFAC-PapersOnLine*, 2020, 53(2):11907-11912.
16. Jing Shi, Yuchen Yao, Jie Bao, Maria Skyllas-Kazacos, Barry J. Welch, Ali Jassim, and Mohamed Mahmoud, A New Control Strategy for the Aluminum Reduction Process Using Economic Model Predictive Control, *IFAC-PapersOnLine*, 2021, 54(11):49-54.
17. Jing Shi, Yuchen Yao, Jie Bao, Maria Skyllas-Kazacos, Barry J. Welch, Ali Jassim, and Mohamed Mahmoud, Advanced Model-Based Estimation and Control of Alumina Concentration in an Aluminum Reduction Cell, *JOM*, 2022, 74(2):706-717.